Electrochemical Sensing with High Aspect Ratio Carbon Nanotube Platforms

Benjamin J. Brownlee and Brian D. Iverson
Department of Mechanical Engineering
Brigham Young University

ABSTRACT

Increased sensitivity of electrochemical sensors is important for detection of low analyte concentrations. A unique flow-through sensor is demonstrated by depositing nanostructured platinum catalyst onto high aspect ratio, porous membranes of vertically-aligned carbon nanotubes (CNTs). Convective mass transfer enhancement was shown to improve the platinum-nanowire-coated CNT (PN-CNT) sensor performance in amperometric sensing of hydrogen peroxide (H_2O_2). Over 90% of the H_2O_2 was oxidized as it passed through the PN-CNT sensor, even for low concentrations in the range of 50 nM to 500 μM. This effective utilization of the analyte in detection demonstrates the utility of exploiting convection in electrochemical sensing. At a 100 μL s^{-1} flow rate, a sensitivity of 24,300 μA mM^{-1} cm^{-2} was achieved based on the frontal projected area, with a 0.03 μM limit of detection and a linear sensing range of 0.03-500 μM. Glucose oxidase was also functionalized unto the surfaces of PN-CNT sensors by polymer entrapment to enable detection of low glucose concentrations.

INTRODUCTION

A vast amount of research has gone into improving the sensitivity of electrochemical sensors in an attempt to detect biomolecules in low concentrations and in low volumes [1]. In particular, glucose detection has widespread appeal as millions of diabetics across the world monitor blood sugar levels daily. Detection of glucose currently involves an invasive prick of the finger, but non-invasive glucose monitoring may be possible by measuring more readily accessible bodily fluids, such as saliva. It has been shown that there is a strong correlation between glucose concentration in blood and glucose concentration in saliva [2]. However, the concentration in saliva is significantly lower, such that a more sensitive glucose sensor is needed to measure glucose levels accurately.

One key aspect to electrochemical sensing is the transport of species from the electrolyte solution to the sensing surface of the electrode. By increasing the mass transport to the electrode, a more sensitive sensor can be produced to allow the detection of lower analyte concentrations. In cases where the analyte concentration is low, transport must be efficient to capitalize on the sparsely available target.

Mass transfer can be increased by increasing the electrode surface area, thereby providing more locations where the analyte can react. However, an increased surface area can also create more noise in the electrical signal. Thus, it is important that the ratio of surface area to solution volume be maximized. This can be done through design of electrode geometry or with electrode surfaces that are enhanced by nanomaterials. Microstructured surfaces, such as 3D graphene [3], greatly increase electrode surface area and have been shown to outperform planar geometries [4].

For flow in a confined geometry such as a channel, concentration boundary layer growth is limited once the boundary layers have merged, resulting in a maximum transport distance of half the channel diameter. These short transport lengths result in high mass transport coefficients, especially as the channel diameter is reduced. The concept of flow-through electrodes originated in the 1970s [5]. However, with recent developments in microfabrication and materials science, the ability to sense target analyte has greatly increased, yet many sensors have not taken advantage of flowing analyte through the sensor. For example, carbon nanotubes (CNTs) have been widely used in electrochemical sensing because of their unique structural, mechanical, and electronic properties [6]. CNTs on supporting membranes have been used as flow-through electrodes for electrochemical filtering [7], but only recently have membrane-supported CNT flow-through electrodes been used for electrochemical sensing [8].

The present work utilizes a high aspect ratio, free-standing membrane (~250 μm height) of vertically aligned carbon nanotubes (CNTs) that form an array of aligned, parallel microchannels (of 4 or 16 μm diameter). This structure was previously used for the decomposition of hydrogen peroxide (H_2O_2) at high concentrations for underwater vehicle propulsion [9]. The CNT walls are coated with platinum nanowires (PNs) to increase the electrocatalytic capability of the sensor during subsequent amperometric sensing of H_2O_2. We demonstrate near complete detection (>90%) of H_2O_2 at concentrations down to 50 nM through exploitation of the sensor geometry and convective enhancement. Glucose oxidase was also functionalized unto the surfaces of PN-CNT sensors by polymer entrapment to enable detection of low glucose

concentrations. Therefore, the CNT sensing platform utilized here offers an efficient method for chemical sensing/biosensing and shows promise for incorporation into the flow field of an electrochemical microfluidic device and larger macroscale flow cells as portrayed in this work.

MATERIALS AND METHODS

Fabrication of the CNT sensing platform followed the methods outlined by Marr et al. [9]. An aluminum oxide (Al_2O_3) film approximately 50 nm thick was deposited on a silicon (Si) wafer using a Denton e-beam evaporator. A 7 nm layer of iron (Fe) was thermally evaporated onto patterned photoresist to achieve two different CNT sensor pore geometries (4 µm and 16 µm diameter microchannels). The wafer was agitated in N-Methyl-2-pyrrolidone (NMP) for at least 10 minutes to remove the patterned photoresist in a lift-off process, resulting in a hexagonally packed arrangement of Fe free regions. The layers of construction for the CNT architecture are illustrated in Fig. 1A.

Diced Fe-patterned wafers were placed in a Lindberg/Blue M Tube Furnace for CNT growth in flowing hydrogen (230 sccm) and ethylene (250 sccm) at 750 °C for 6 minutes. After 6 minutes of growth, the multi-walled CNTs achieved a height of about 250 µm with diameters on the order of 20 nm (see Fig. 1B). To create a stronger, agglomerated structure, the CNTs were coated (infiltrated) with amorphous carbon in the furnace by flowing hydrogen (158 sccm) and ethylene (250 sccm) at 900 °C for 10 minutes (see Fig. 1C). This infiltration/coating process with amorphous carbon results in the attachment of neighboring CNTs and enables a mechanically robust yet porous array of microchannels (see Fig. 1D). The hydrogen gas during carbon infiltration allows the CNT microstructure to self-release from the Si substrate, creating a stand-alone microstructure comprised of carbon-coated, CNT walls (see Fig. 1E).

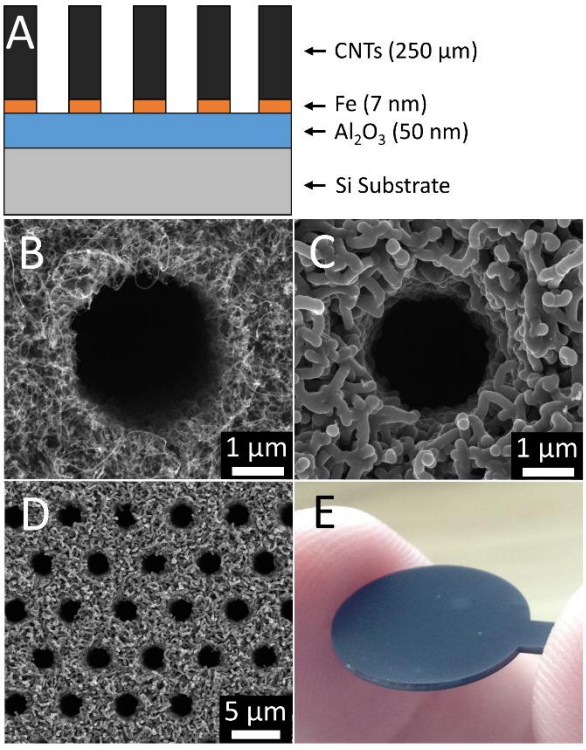

Fig. 1. (A) Schematic of layers used to manufacture the CNT sensor architecture. Scanning electron microscope (SEM) images of CNTs that form microchannels with a nominal 4 µm diameter (B) immediately after growth, (C) coated with amorphous carbon after infiltration, and (D) an array of porous-walled-microchannels aligned with the direction of the bulk CNT growth. (E) Sample CNT sensor after self-release from the Si substrate.

Although the CNT membranes self-released from the wafers, the side closest to the Si substrate was covered by a thin carbon layer during infiltration. To remove this layer, an oxygen (O_2) plasma etch was performed for 5 minutes in an Anelva Reactive Ion Etcher DEM-451 (300 W, 3.1 sccm O_2). An additional 2 minute etch was performed on the top face of the released structure to render the carbon surfaces hydrophilic.

Platinum nanowires (PNs) were deposited onto the CNT sensors in a static, electroless environment using a chemical reduction of chloroplatinic acid hexahydrate (37.5% Pt, Sigma-Aldrich 206083) similar to previous protocols [9, 10]. The concentration used in each deposition was dependent on the mass of the CNT sensor, with a target of 30% Pt to carbon weight in solution (2.9 ± 0.4 mM chloroplatinic acid). Each CNT sensor was held vertically in a Teflon stand for 24 hours in a solution containing chloroplatinic acid, 18 mL of ultrapure water and 2 mL of formic acid (88% HCOOH, Macron 2592-05). After the deposition, the samples were soaked in deionized water for 5 minutes and then placed in a dehydration oven for 10 minutes. The resulting Pt coverage on the CNTs is shown in Fig. 2.

For the functionalized glucose sensors, glucose oxidase from *Aspergillus niger* (GOx, type X-S, 100,000-250,000 units/g, G7141 Sigma-Aldrich) was entrapped in the polymer poly(3,4-ethylene-dioxythiophene) (PEDOT) at the CNT surfaces following a procedure similar to that of Claussen et al. [11]. First, 105 mg of poly(sodium 4-styrenesulfonate) (PSS, Sigma Aldrich 243051) was stirred into 15 mL of ultra-pure water. Then, 48 µL of 3,4-ethylene-dioxythiophene (EDOT, Sigma Aldrich 483028) was mixed into the PSS solution. Finally, 75 mg of GOx (5 mg/mL) was added to the EDOT-PSS solution. This 15 mL mixture allowed for the electropolymerization of EDOT to PEDOT in a stirred (100 rpm) 20 mL beaker with the PN-CNT sensor as the working electrode, a 25 mm square platinum gauze (80 mesh) counter

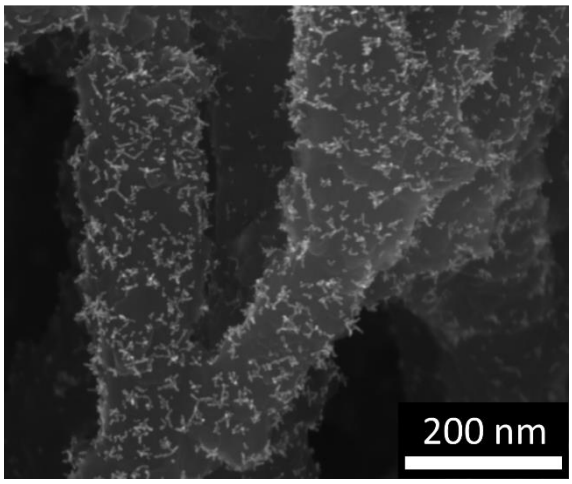

Fig. 2. SEM image of platinum coverage on CNTs as found near the axial center of the microchannel.

electrode, and a saturated (in KCl) silver/silver chloride (Ag/AgCl) reference electrode. A CHI 660 Potentiostat/Galvanostat (operating in multi-current step mode) passed through 500 one second cycles, with 0.5 seconds at 1.05 mA and 0.5 seconds at 0 A.

Amperometric sensing experiments were performed using the same equipment as in the electropolymerization, except a platinum wire was used in place of the platinum gauze for the counter electrode. The potential of the PN-CNT sensor was held constant at 650 mV relative to Ag/AgCl. Before experiments were performed, this potential was applied until a steady baseline current was achieved from the buffer solution alone.

Both H_2O_2 and glucose were detected to illustrate the influence of convection and mass transfer on chemical sensing. Electrical current was produced from the oxidation reaction of H_2O_2. Glucose was broken down into H_2O_2 with GOx, from which a current was generated, as shown in the following two equations:

$$\text{D-glucose} + O_2 + H_2O \rightarrow \text{D-gluconic acid} + H_2O_2$$

$$H_2O_2 \rightarrow O_2 + 2H^+ + 2e^-$$

Two electrons correspond to one molecule of oxidized H_2O_2, allowing the direct correlation between current and oxidation rate using the rate form of Faraday's law,

$$N = \frac{I}{nF}$$

where N is the molar oxidation rate of H_2O_2 (mol s^{-1}), I is the current (A), n is the moles of electrons per mole of H_2O_2, and F is Faraday's constant.

The flow-through electrochemical cell is illustrated in Fig. 3. From an upstream reservoir, 50 mL of PBS (or pre-mixed PBS and 30 mg of GOx) was

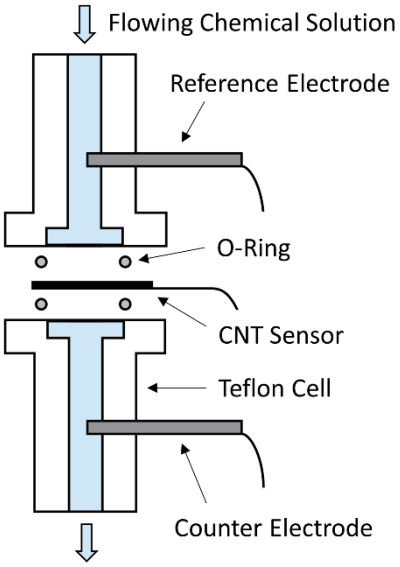

Fig. 3. Exploded view schematic of three electrode through-flow cell, where the chemical solution is forced through the PN-CNT microchannels.

forced through the PN-CNT microchannels. The PN-CNT sensor was clamped together between two O-rings in a machined Teflon flow cell, shown in the exploded view in Fig. 3. This configuration allowed forced mechanical contact between the sensor and a Nichrome wire. The flow cell was oriented vertically, with the reference electrode upstream and the counter electrode downstream of the PN-CNT sensor. A 60 mL syringe pulled the solution through the cell using a Harvard Apparatus PHD Ultra syringe pump to control the flow rate.

RESULTS AND DISCUSSION

The PNs deposited onto the CNT surfaces resulted in a 13.1 ± 3.9 platinum to carbon weight percent. The PN-CNT sensors were 260 ± 48 µm in thickness, yielding aspect ratios (channel length/diameter) of about 16 and 65 for the 16 and 4 µm diameter channels, respectively.

Fig. 4 shows the current response in time from a typical flow through configuration with a 16 µm channel PN-CNT sensor. The baseline currents for different flow rates (10, 25, 50, 75, and 100 µL s^{-1}) were monitored in one minute intervals, but there was little observed change in current due to flow rate. At 300 seconds, 3% H_2O_2 by weight (0.89 M H_2O_2) was added to the upstream reservoir (and quickly stirred together) to obtain a target concentration of 100 µM H_2O_2. This injection of H_2O_2 caused an immediate spike in measured current, which was monitored for three minutes (300 to 480 seconds in Fig. 4). Then, the same flow rates were stepped through in reverse order over

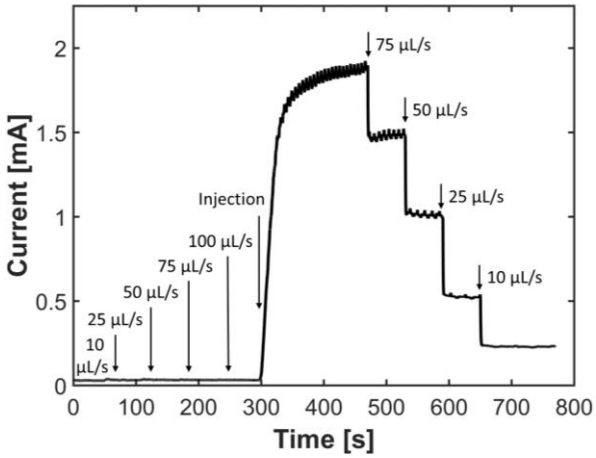

Fig. 4. Through-flow current in time for the 16 µm diameter channel PN-CNT sensor in response to 100 µM H_2O_2 (injected at 300 seconds) at different flow rates (10-100 µL s^{-1}).

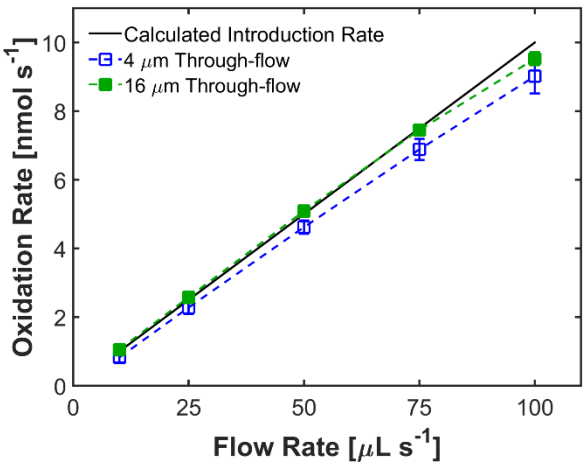

Fig. 5. Through-flow oxidation rates in response to 100 µM H_2O_2 at different flow rates for both 4 and 16 µm diameter channels are compared to the calculated introduction rates of H_2O_2. Error bars represent the standard deviation of three measurements.

one minute intervals until the cell returned to its initial flow rate (10 µL s^{-1}).

The measured currents obtained with the flow-through arrangement were significantly higher than currents previously obtained in stirred experiments [12]. There was a significant increase in current because the microchannels kept the H_2O_2 close to the surface (where the reaction takes place), limiting the concentration boundary layer growth. The volumetric flow rate was a dominant controlling feature of the measured current, as there are sharp drops in current when the flow rate was lowered. The oscillations in the current observed after the injection of H_2O_2 (Fig. 4, after 300 seconds) correspond to the frequency of stepping in the syringe pump. This sensitivity to stepping in the syringe pump motor further indicates the dependence of the measured current on the convective environment, as slight changes in the flow rate caused by the syringe pump resulted in signal oscillations.

The measured oxidation rates for the through-flow experiments are shown in Fig. 5, where three PN-CNT sensors were used for each microchannel diameter to obtain the standard deviation of the response. These oxidation rates are compared to the calculated introduction rates of H_2O_2 into the flow cell, which were determined from the known concentration of H_2O_2 and the volumetric flow rates. The introduction rate is the theoretical maximum oxidation rate at any given flow rate. The 16 µm channel geometry obtained oxidation rates that were nearly identical to the introduction rates (with a slight drop to 95% at 100 µL s^{-1}). This signifies that nearly all the H_2O_2 was oxidized as it passed through the PN-CNT sensor. The 4 µm diameter channels had slightly lower oxidation rates at about 90% of the introduction rate. Oxidation rates for both geometries appeared to increase linearly with flow rate.

The 16 µm diameter PN-CNT sensor at a flow rate of 100 µL s^{-1} provided the highest oxidation rate when tested at 100 µM H_2O_2. Therefore, this geometry and convective environment were chosen to determine the sensitivity, limit of detection (LOD) and linear range for the sensor approach. Fig 6A-C shows the complete linear range of the PN-CNT sensor, in the range of 50 nM to 500 µM, with the oxidation rates remaining linear over about 90% of the introduction rates.

The linear range can be seen at lower concentrations in Fig. 6C. The measured oxidation rates are very close to the introduction rates at these low concentrations, which is particularly useful in the detection of very low concentrations where it is desired to maximize the signal from the available analyte. Fig. 6D shows the current measured in time for the oxidation rates shown in Fig. 6C, at increments of 50 nM. The limit of detection (LOD) at 100 µL s^{-1} was 0.03 µM (using a signal to noise ratio of S/N = 3). Thus, Fig. 6C shows that the PN-CNT sensor is approaching the LOD while still remaining very linear. The linear range is then 0.03 – 500 µM H_2O_2.

The sensitivity (current/molarity) of the PN-CNT sensor was determined to be 17,300 µA mM^{-1}. Normalizing by the 2D surface area similar to other researchers (frontal projected area = 0.713 cm^2) gives a sensitivity of 24,300 µA mM^{-1} cm^{-2}. This is an extremely high sensitivity compared to the typical sensitivity of about 200-2,000 µA mM^{-1} cm^{-2}. If one were to include the nominal microchannel surface area in the normalization (19.86 cm^2), a sensitivity of 871 µA mM^{-1} cm^{-2} would be obtained.

For the maximum flow rate of 100 µL s^{-1}, the average velocity through the microchannels was only 0.34 cm s^{-1}, about 1% of the relative fluid velocity found in a stirred electrochemical cell (with a stir speed

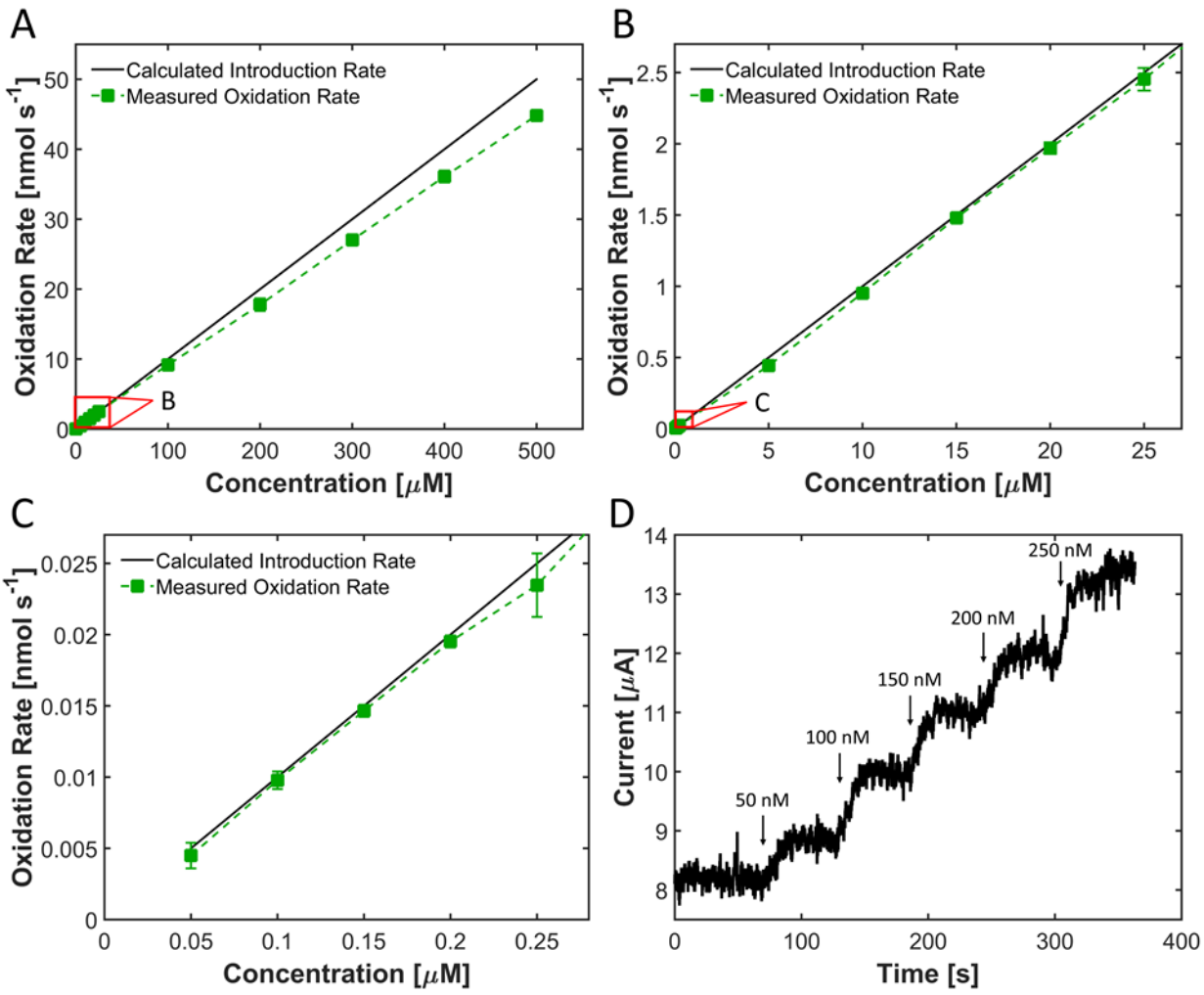

Fig. 6. (A) Linear range of 16 µm diameter PN-CNT sensor at a flow rate of 100 µL s^{-1}. (B) Close up linear range of (A) up to 25 µM. (C) Close up linear range of (B) up to 0.25 µM. This linear range is approaching the limit of detection of 0.03 µM. (D) The current measured in time for additions of 50 nM H_2O_2, which were used to determine the oxidation rates obtained in (C). In all cases, error bars represent the standard deviation of three measurements.

of about 500 rpm [12]). The drastic improvement in measurement signal for the through-flow configuration, despite lower average velocities, is due to the intimate contact between analyte and sensing surface achieved through limiting the concentration boundary layer by forcing the liquid through the sensor architecture.

A major factor that limited the upper end of the sensing range was the formation of oxygen bubbles due to the high oxidation rates of H_2O_2. Because the experiments were performed by withdrawing the syringe pump, the resulting bubbles in the liquid line had the potential to cause discontinuity in the measured signal. An alternative approach would be to perform the experiments with infusion pumping, such that the generated gases are swept toward a free surface and do not obstruct the signal at high H_2O_2 concentrations.

The detection limit of the PN-CNT sensor could potentially be improved by increasing the flow rate above 100 µL s^{-1} to obtain higher current responses for the same H_2O_2 concentration. It appeared that slight variations in the Pt coverage had little effect on the sensor signal; however, samples without Pt had a very low response with <2% of the measured oxidation rate for PN-CNT sensors at 100 µL s^{-1}.

The glucose sensors with GOx entrapped in PEDOT on the PN-CNT (PEDOT-PN-CNT) surfaces were tested at the same flow rate of 100 µL s^{-1}. The measured current in response to 100 µM and 1 mM glucose is shown in Fig. 7. In both cases there was a spike in current immediately after the glucose injection, after which the current leveled out at a higher value than before the injection.

Although there was a good response to glucose at 100 µM, the measured current was significantly lower than the measured current in response to H_2O_2 at the same concentration. Thus, to identify a target maximum

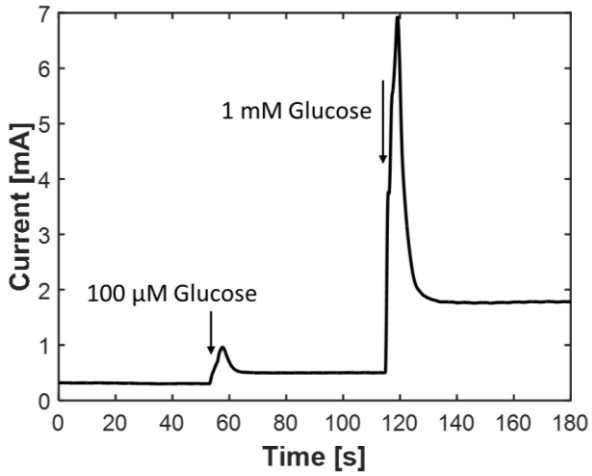

Fig. 7. Current measured in response to 100 µM and 1 mM glucose using PEDOT-PN-CNT sensors with a 100 µL s^{-1} flow rate.

current for the detection of glucose at a given concentration, glucose oxidase was mixed into the PBS solution prior to sensing glucose using PN-CNT sensors (without GOx in PEDOT). This allowed for the glucose to be oxidized before reaching the PN-CNT sensor and theoretically approach the maximum achievable current.

Similar to H_2O_2, the measured current can be used to calculate the oxidation rate. Fig. 8 shows a comparison of the oxidation rates for glucose detection with PEDOT-PN-CNT sensors and for GOx pre-mixed into the PBS solution, both of which are compared to the calculated introduction rate for 100 µM glucose at 100 µL s^{-1}. The mixed scenario gave an oxidation rate that was about half of the introduction rate, while the PEDOT-PN-CNT sensor gave only about 10% of the introduction rate. This shows that the maximum detection of glucose would be half of the glucose that

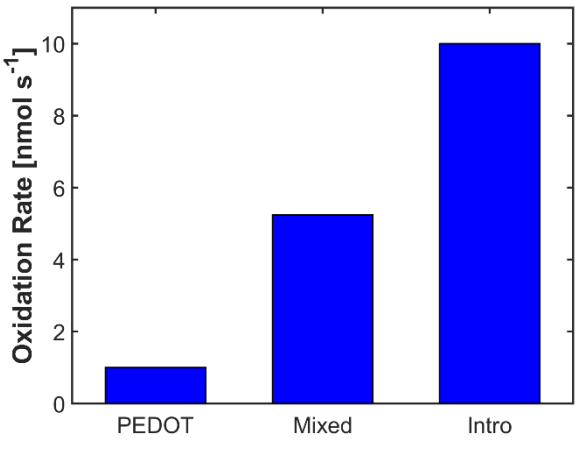

Fig. 8. Comparison of oxidation rates for the PEDOT-PN-CNT sensor and pre-mixed GOx in the PBS solution, both of which are compared to the calculated introduction rate for 100 µM glucose at 100 µL s^{-1}.

passed through the sensor, possibly due to some inefficiencies in the conversion to H_2O_2 using GOx. The PEDOT-PN-CNT sensor was even lower, possibly due to transport restrictions through the polymer or to poor coverage of GOx and PEDOT within the microchannels. Thus, future work will look at improving the coverage of GOx within the microchannels, either by variations of polymer entrapment or by covalent bonding.

CONCLUSION

This work highlights the utility of convection in detecting low analyte concentrations. We have shown how high aspect ratio PN-CNT sensors provide a unique sensing platform that enhances mass transfer by enabling high surface area and confining concentration boundary layers. PN-CNT sensor performance was measured by the amperometric sensing of H_2O_2 and glucose, where it was shown that convection had a significant influence on the measured current. Over 90% of the H_2O_2 was oxidized as it passed through the PN-CNT sensor, producing high currents at low velocities. The large current response obtained by flow through the PN-CNT microchannels resulted in a very high sensitivity, allowing for the detection of H_2O_2 concentrations in the nM range. Glucose detection was possible at low concentrations but was shown to be less effective than H_2O_2, suggesting that potential future work could include investigating the effect of increasing coverage of GOx in the microchannels.

REFERENCES

[1] L. Nyholm, Electrochemical techniques for lab-on-a-chip applications, Analyst, 130 (2005) 599-605.

[2] S. Gupta, S.V. Sandhu, H. Bansal, D. Sharma, Comparison of Salivary and Serum Glucose Levels in Diabetic Patients, Journal of Diabetes Science and Technology, 9 (2015) 91-96.

[3] S. Sattayasamitsathit, Y. Gu, K. Kaufmann, W. Jia, X. Xiao, M. Rodriguez, et al., Highly Ordered Multilayered 3D Graphene Decorated with Metal Nanoparticles, Journal of Materials Chemistry A, 1 (2013) 1639-1645.

[4] F. Schröper, D. Brüggemann, Y. Mourzina, B. Wolfrum, A. Offenhäusser, D. Mayer, Analyzing the electroactive surface of gold nanopillars by electrochemical methods for electrode miniaturization, Electrochimica Acta, 53 (2008) 6265-6272.

[5] R. Alkire, B. Gracon, Flow-Through Porous Electrodes, Journal of The Electrochemical Society, 122 (1975) 1594-1601.

[6] C. Gao, Z. Guo, J.-H. Liu, X.-J. Huang, The new age of carbon nanotubes: An updated review of functionalized carbon nanotubes in electrochemical sensors, Nanoscale, 4 (2012) 1948-1963.

[7] M.H. Schnoor, C.D. Vecitis, Quantitative Examination of Aqueous Ferrocyanide Oxidation in a Carbon Nanotube Electrochemical Filter: Effects of Flow Rate, Ionic Strength, and Cathode Material, The Journal of Physical Chemistry C, 117 (2013) 2855-2867.

[8] A. Buffa, Y. Erel, D. Mandler, Carbon Nanotube Based Flow-Through Electrochemical Cell for Electroanalysis, Analytical Chemistry, 88 (2016) 11007-11015.
[9] K.M. Marr, B. Chen, E.J. Mootz, J. Geder, M. Pruessner, B.J. Melde, et al., High Aspect Ratio Carbon Nanotube Membranes Decorated with Pt Nanoparticle Urchins for Micro Underwater Vehicle Propulsion via H2O2 Decomposition, ACS Nano, 9 (2015) 7791-7803.
[10] J.C. Claussen, M.A. Daniele, J. Geder, M. Pruessner, A.J. Makinen, B.J. Melde, et al., Platinum-Paper Micromotors: An Urchin-Like Nanohybrid Catalyst for Green Monopropellant Bubble-Thrusters, ACS Applied Materials & Interfaces, 6 (2014) 17837-17847.
[11] J.C. Claussen, A. Kumar, D.B. Jaroch, M.H. Khawaja, A.B. Hibbard, D.M. Porterfield, et al., Nanostructuring Platinum Nanoparticles on Multilayered Graphene Petal Nanosheets for Electrochemical Biosensing, Advanced Functional Materials, 22 (2012) 3399-3405.
[12] B.J. Brownlee, K.M. Marr, J.C. Claussen, B.D. Iverson, Improving sensitivity of electrochemical sensors with convective transport in free-standing, carbon nanotube structures, Sensors and Actuators B: Chemical, 246 (2017) 20-28.